

# MICROBIALS

## BACTERIAL COLONIZATION OF SURFACES IN FLOWING SYSTEMS: METHODS AND ANALYSIS

**S**urfaces in flowing systems are subject to colonization by bacteria (1). Adsorbed bacteria are a potential source of contamination for any material that contacts the surface, a consideration of importance in pure-water systems. This article describes an experimental strategy for studying initial events in bacterial colonization of surfaces. The experimental goal is to identify surface features that affect the rate and pattern of bacterial adsorption. Greater understanding of these factors could lead to improved control of bacterial adsorption and therefore of process stream contamination.

Several quantitative theories for bacterial adsorption have been proposed by others. In brief, these theories discriminate between two types of bacterial adsorption: physical adsorption, and chemisorption or adhesion (2,3). Physical adsorption is a reversible or equilibrium adsorption involving primary physical forces. Chemisorption is generally irreversible and is the result of short-range forces, including chemical bonds, dipole interactions, and hydrophobic bonding.

Some theoretical structures permit the possibility that an adsorbed cell either inhibits or enhances the adsorption of other cells nearby. These two opposite

effects have been termed *blocking* and *positive cooperativity*, respectively (4,5). Under blocking, the initial colonizing cells would position themselves in a regular pattern, with few near neighbors. Under cooperativity, the initial colonizing cells would be arrayed in an aggregated pattern with many near neighbors. Some recent research on bacterial adsorption has been directed at measuring these two effects by observing the spatial patterns of surface-colonizing bacteria (6-8).

Our experiments do not involve any of these conventional theories. Instead, we hope to uncover empirical relationships between bacterial adsorption locations and physical/chemical surface characteristics. In order to arrive at an empirical description, we had to devise novel procedures for viewing the colonization process and quantifying the data. The purposes of this article are to describe our methodology and to present some preliminary results.

### Materials and Methods Stainless steel coupon.

Figure 1 shows the steps in our experimental protocol. The test substratum consisted of a 12.7- by 6.35-millimeter (mm) 316L stainless steel coupon, either electropolished (Experiment 2), or electropolished and further hand-polished with 0.3-micron ( $\mu\text{m}$ ) alumina grit to a mirror finish (Experiment 1). A 7 X 7 grid of points was laser-etched (Texas Laserworks, Waco, Texas) onto the coupon surface. The points were approximately 5  $\mu\text{m}$  deep, 10  $\mu\text{m}$  in diameter, and marked at 50- $\mu\text{m}$  intervals, so that the grid defined a 6 X 6 matrix of contiguous squares, each square 50  $\mu\text{m}$  on a side. The total 300 X 300  $\mu\text{m}$  area formed our observation region.

The grid points were used

as reference points to register (overlay) images from the confocal scanning laser microscopy (CSLM), atomic force microscopy (AFM), and Auger spectroscope (AS); and to connect the separate 50- $\mu\text{m}$ -square images to form a larger square (see Image Acquisition, below). Before placing the coupon in the flow cell, the surface topography within selected grid squares was characterized by AFM. In subsequent experiments, an elemental mapping of the surface chemistry in those same squares was recorded using Auger spectroscopy.

**Flow cell.** The flow cell consisted of two parallel flat plates. The top plate allowed for a large glass coverslip that served as an observation window, and the bottom contained a recessed well for the coupon. Overall chamber dimensions were 40 mm long by 12 mm wide by 0.01 mm thick. Flow conditions were maintained at a Reynold's number of 6 and a shear stress at the coupon surface of 0.75 newtons per meter squared ( $\text{Nm}^{-2}$ ). The

By Anne K. Camper,  
Martin A. Hamilton, Ph.D.,  
Kirk R. Johnson,  
Paul Stoodley,  
Gary J. Harkin, Ph.D.  
and Don S. Daly  
Center for Biofilm Engineering  
Montana State University

ISSN:0747-8291. COPYRIGHT (C) Tall Oaks Publishing, Inc. Reproduction in whole, or in part, without permission of publisher is prohibited. Those registered with the Copyright Clearance Center (CCC) may photocopy this article for a flat fee of \$1.50 per copy.

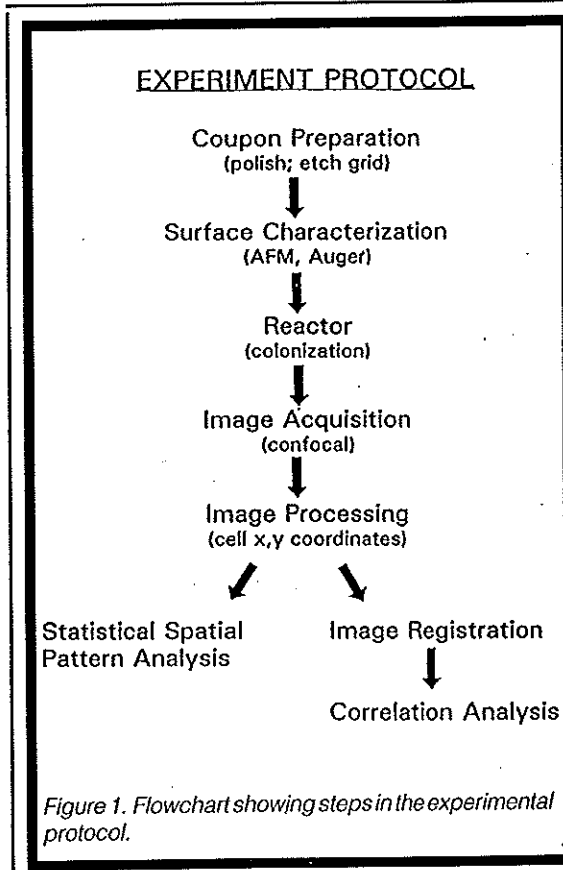
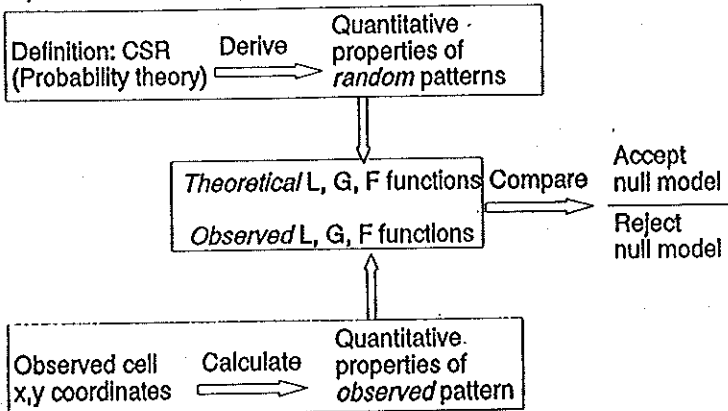


Figure 1. Flowchart showing steps in the experimental protocol.

NULL MODEL: Complete Spatial Randomness (CSR)



DATA

Figure 2. Flowchart describing the statistical screening test.

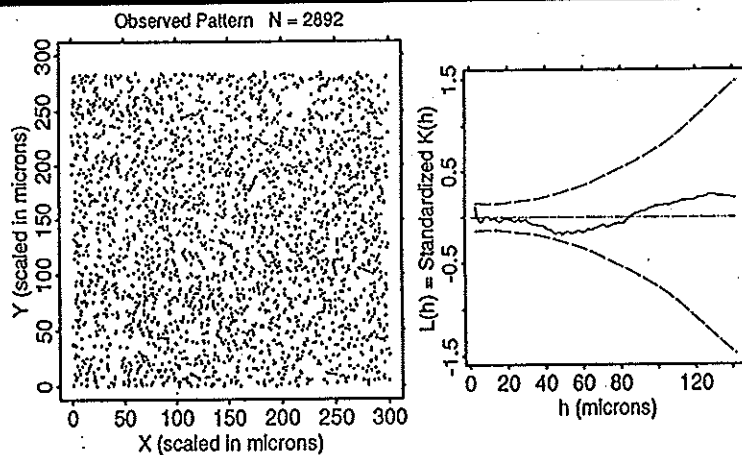


Figure 3. Pattern of bacterial adsorption and the associated SPPA; *P. aeruginosa* on a 316L stainless steel surface at 99 minutes. The steel surface was electropolished and then hand-polished with 0.3 alumina grit (Experiment 1). Under the null hypothesis (CSR pattern), the theoretical value of the plotted L function is identically zero, and the tolerance envelope would completely enclose a realization of the L function with probability 99%.

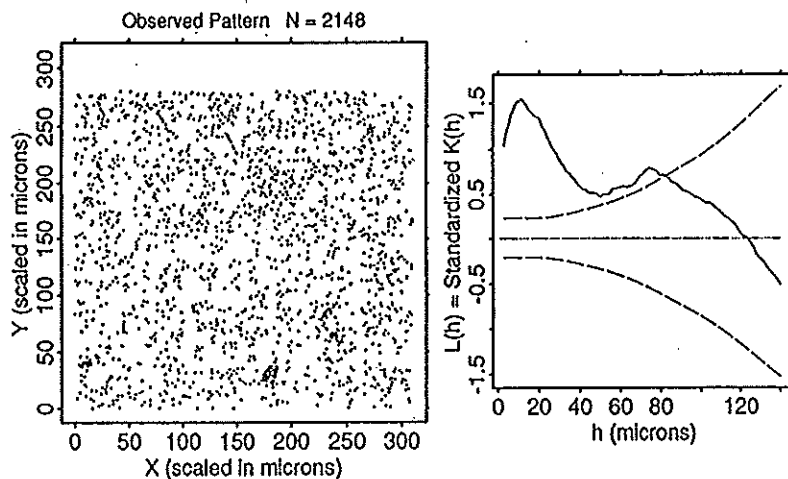


Figure 4. Pattern of bacterial adsorption and the associated statistical SPPA; *P. aeruginosa* on a 316L stainless steel surface at 99 minutes. The steel surface was electropolished (Experiment 2). Same interpretation as in Figure 3.

entire flow cell was autoclaved before inserting the coupon, which had been sterilized using ultraviolet light prior to inoculation.

**Inoculum preparation.** The test organism was a *Pseudomonas aeruginosa* originally isolated from an industrial biofilm. It was grown in a chemostat with a residence time of 5 hours. Sterile influent feed contained (per liter of distilled water) 0.1 gram (g) glucose, 0.7 g dibasic potassium phosphate ( $K_2HPO_4$ ), 0.3 g monobasic potassium phosphate ( $KH_2PO_4$ ), 0.1 g ammonium sulfate ( $(NH_4)_2SO_4$ ), and 0.01 g magnesium sulfate ( $MgSO_4 \cdot 7H_2O$ ). Chemostat effluent, diluted with the same medium without glucose to provide  $10^8$  cells per milliliter (mL), was pumped through the flow cell.

**Image acquisition.** The adsorption of individual cells to the coupon surface within the observation region was observed nondestructively and in real time by reflected light imaging of 1,000 magnification, using a BioRad MRC 600 CSLM associated with an Olympus BH-2 microscope. Images of colonizing bacteria were collected systematically across each grid square. Total image acquisition and storage time for nine consecutive images was 10 minutes. When a time series for a sample area was desired, the image capture procedure was repeated at defined time intervals.

**Image processing.** Following the completion of an experiment, individual images were displayed on a computer monitor. The x,y positions of all bacteria and the four laser-etched corner points were identified using in-house image-analysis software. Those positions were stored in a computer file for statistical analysis.

**Statistical analysis.** Suppose that the pattern exhibited by bacteria colonizing a smooth surface (Experiment 1) represents the "inherent biological" colonization pattern for our strain of *P. aeruginosa*. If so, then the colonization patterns on surfaces of increasing topographic and chemical heterogeneity (e.g., Experiment 2) may indicate that there exists a level of heterogeneity at which the colonizing bacteria form a different pattern. By correlating bacterial adsorption sites with physical/chemical maps of the surface, we hope to uncover the factors causing the new pattern. The statistical

analysis comprises two steps: screening patterns for departure from the inherent biological pattern, and correlating the locations of bacterial adsorption with surface features.

### Screening for Nonrandom Patterns

We believe the inherent colonization pattern for *P. aeruginosa* is completely spatially random (CSR). (In the language of stochastic modeling, CSR means that the  $x,y$  positions of the adsorbing bacteria can be modeled as a two-dimensional, homogeneous Poisson distribution.) We conjectured that chemical and topographic heterogeneities would be patchy; if bacterial adsorption were affected by those heterogeneities, the result would be aggregated patterns of adsorbed bacteria.

We have found that statistical spatial point pattern analysis (SPPA) based on distance functions is particularly useful for discriminating CSR from aggregated patterns (9-11). To our knowledge, statistical SPPA has never before been applied in bacterial surface colonization studies, perhaps because SPPA requires a map of the locations of adsorbing bacteria, which in turn requires a sophisticated image analysis system.

It is important to control the risk of *false significance* for the screening tests; consequently, we have constructed a test based on SPPA that holds the risk of false significance to a small, known value. This test has been fully described elsewhere (12). Figure 2 shows the steps involved.

In brief, the map of positions of adsorbed bacteria is converted into three distance functions: L, F, and G. The function L(h) is a standardized measure of relative crowding within a circle of radius h ( $\mu\text{m}$ ). The function F(h) is the cumulative distribution function of the distance between a random point and the nearest adsorbed bacterium to that random point. The function G(h) is the cumulative distribution function of the distance between an adsorbed bacterium and its nearest neighbor. The functions F and G are particularly useful for looking at small-scale patterns (distances less than 10  $\mu\text{m}$ ), and L is useful for finding patterns on a larger scale (up to 150  $\mu\text{m}$  for our experiments). Because we expected the stainless steel surface features to exhibit patchiness on the larger scale, we relied particularly on the L function for screening purposes, and only the L function will be discussed below.

For presentation of the results, the L function is plotted, with distance on the abscissa (the x-axis) and L on the ordinate (the y-axis). If the data exactly corresponded to the null hypothesis (CSR), the observed L would be flat at ordinate zero. Even if the null hypothesis were true, however, we expect the observed L to differ from zero because of statistical variability. An assessment of statistical variability is shown in our plots by *tolerance envelopes*. The distance function attains statistical significance at level  $\alpha$  if the observed function crosses the  $100(1-\alpha)\%$  tolerance envelope. We have chosen to construct the 99% envelopes for this article.

### Correlation Analysis

Here *correlation analysis* designates the goal of determining whether the positions of the bacteria are associated with surface topography or with surface chemistry. To accomplish this goal, it is necessary to quantify topographic features. There are many potential quantifiable factors, including altitude, slope, aspect relative to the direction of flow,

and combinations of such factors.

For this discussion, we will focus on altitude as measured by the pixel intensity in the AFM image: specifically, the altitude value attached to any pixel position  $x,y$  in the AFM image was calculated by averaging the pixel intensity over the 5 X 5 square of pixels centered at  $x,y$ . In this context, we decided that cell positions were associated with topography if the distribution of altitudes at bacteria locations was statistically significantly different from the distribution of altitudes for the overall image.

The analysis began by registering the AFM image to the CSLM image for a specific grid square. A specific area of interest (AOI) within the square was selected to exclude the laser-etched grid dots. The cumulative distribution function of altitudes over the AOI was calculated; A denoted that function. Then the  $x,y$  positions of adsorbed bacteria were plotted on the registered AFM image and N denoted the number of bacteria. The cumulative distribution of the associated N altitudes was calculated;  $A_b$  denoted that function. The standard-

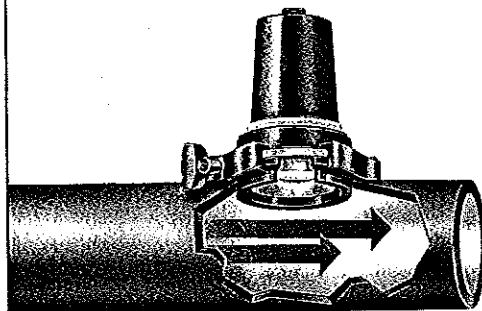
## We measure pressure in line ...

with our new flush mounted Model 560 pressure transmitter, that connects directly in line with a variety of adapters.

To insure the integrity of an ultrapure water system, the wetted surface of the 560 is constructed of PVDF and a ceramic sensing diaphragm. Contamination won't leech into the system!

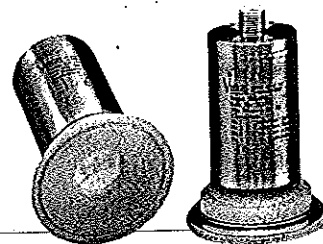
Viatran continues to develop products to meet your pressure measurement needs.

Call us today.



**Viatran**  
CORPORATION

300 INDUSTRIAL DRIVE  
GRAND ISLAND  
NEW YORK 14072  
PHONE 800-688-0030  
FAX 716-773-2488



CIRCLE READER SERVICE CARD NO. 20

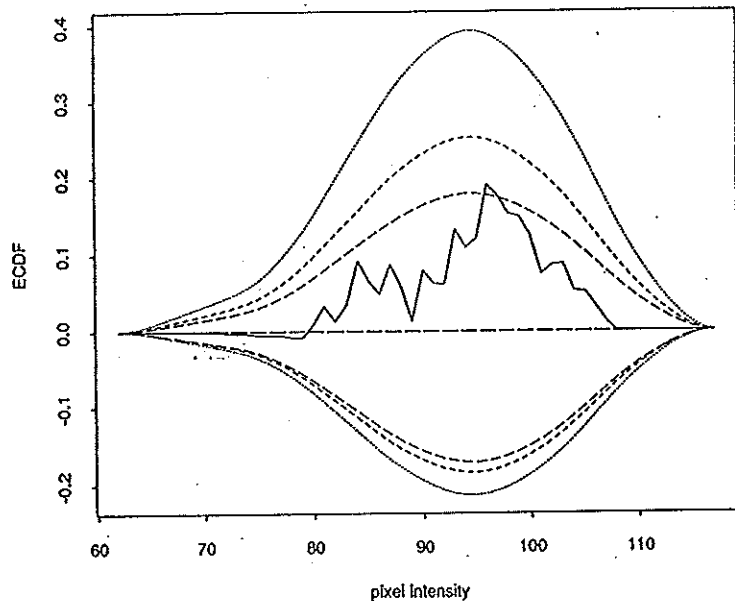


Figure 5. The ECDF plot for assessing the association between topographic altitude and positions of adsorbing bacteria in a  $50 \times 50 \mu\text{m}$  subsquare; *P. aeruginosa* on a 316L stainless steel surface at 99 minutes. The steel surface was electropolished (duplicate run of Experiment 2). Under the null hypothesis of no association, the theoretical value of the plotted ECDF function is identically zero, and the three tolerance envelopes would completely enclose a realization of the ECDF function with probabilities of 90%, 95%, and 99%, respectively.

ized difference between the functions,  $\text{ECDF} = (A_0 - A)/\text{SE}$ , where SE, the standard error of  $(A_0 - A)$ , was calculated exactly as described in Hamilton et al. (12) for the L function.

The calculation required 200 computer simulations of the adsorption process under the null hypothesis that bacteria positions are independent of altitude. For each simulation,  $N$  points were selected at random within the AOI, and the associated cumulative distribution function for altitudes was calculated.

The results of the analysis were plotted with altitude on the abscissa; and the standardized difference, ECDF, on the ordinate. The interpretation is as described for the L function screening test. If the data exactly corresponded to the null hypothesis, the plot would be flat at ordinate zero. The extent of statistical variability is indicated by tolerance envelopes. The ECDF attains statistical significance at level  $\alpha$  if the observed ECDF crosses the  $100(1-\alpha)\%$  tolerance envelope. We have chosen to show 90%, 95%, and 99% envelopes for the ECDF.

### Results

Experiment 1 used a topographically homogeneous surface (electropolished and hand-polished); it provides control data to which experiments using hetero-

geneous surfaces can be compared. Figure 3 shows the Experiment 1 adsorption pattern in the left-hand panel and the associated L function in the right-hand panel. The observed L function lies well inside the 99% tolerance envelope, and there is no evidence that the bacteria form a non-CSR pattern. Consequently, we have not conducted a correlation analysis of Experiment 1 data.

Experiment 2 used a coupon with a slightly rougher surface (electropolished only). Figure 4 shows the results. The observed L function crossed outside the upper envelope, indicating statistically significant aggregation ( $\alpha$  less than or equal to 0.01). The bacterial pattern clearly shows areas of aggregation. Consequently, we have begun a correlation analysis, which is being conducted at the time of writing. Figure 5 shows the ECDF plot for one  $50 \times 50 \mu\text{m}$  square from a duplicate run of Experiment 2. The observed function crosses the 90% envelope, but not the 95% envelope; therefore, there is a weakly significant association between bacteria positions and altitude in this square.

### Discussion

Other distance functions have been used in microbial adsorption studies. Busscher and his colleagues (4, 6, 13)

have mapped positions of adhering bacteria in flowing systems and calculated two distance functions, which they call the *radial distribution function* and the *angular distribution function*. The radial distribution function is related to the derivative of L. The angular distribution function accounts for possible effects of the direction of flow. Busscher et al. (14) recently proposed a general *pair distribution function* that contains information for calculating the angular distribution function for any angle. All of these functions are used for local pattern analysis only, and they have been interpreted within the conventional theories reviewed at the beginning of this article. Although no statistical methodology has been developed for these functions, our tolerance envelope methodology would be appropriate.

**Work in progress.** Experiments have been conducted with rougher surfaces (e.g., 320-grit mechanically polished 316L stainless steel) and with other species of bacteria. The correlation analysis can be applied to Auger images (surface chemistry) as well as to AFM images. We are developing a statistical multiple regression technique suitable for describing the rate of bacterial adsorption as a function of surface topography and chemistry. The software is designed but not written. We anticipate that these analyses will lead to a generalized Poisson process model for cell adsorption in which the Poisson intensity parameter is a function of topography and/or chemistry.

### Conclusions

The experimental protocol has been successfully carried out. Software for registering images from different microscopes, quantifying the images, and performing statistical tests has been completed, but only preliminary results are available. We observed no departure from CSR on the electro- and hand-polished surface, but found statistically significant aggregation on the electropolished-only surface. We believe this research strategy has the potential for elucidating important factors affecting bacterial adsorption to surfaces in a flowing system. The technique can be applied to a broad spectrum of substrata, flow conditions, and bacteria consortia. ■

### Acknowledgments

This research was supported in part by Cooperative Agreement ECD-8907039

between the National Science Foundation and Montana State University, and by the Industrial Associates of the Center for Biofilm Engineering.

#### References

1. Mallysse, A.G. "Adhesion, Bacterial", in *Encyclopedia of Microbiology*, Vol. 1, pp. 29-36, Academic Press, San Diego, Calif. (1992).
2. Characklis, W.G.; Marshall, K.C. *Biofilms*, John Wiley & Sons Inc., New York, N.Y. (1990).
3. Marshall, K.C. "Mechanisms of Bacterial Adhesion at Solid-water Interfaces", *Bacterial Adhesion-Mechanisms and Physiological Significance*, Savage D.C.; Fletcher, M., Eds., pp. 133-161, Plenum Publishing Corp., New York, N.Y. (1985).
4. Busscher, H.J.; Doornbusch, G.I.; Van Der Mei, H.C. "Adhesion of Mutans Streptococci to Glass with and without a Salivary Coating as Studied in a Parallel-plate Flow Chamber", *Journal of Dental Research*, 71, pp. 491-500 (March 1992).
5. Doyle, R.J.; Nesbitt, W.E.; Taylor, K.G. "On the Mechanism of Adherence of Streptococcus Sanguis to Hydroxylapatite", *FEMS Microbiological Letters*, 15, pp. 1-15 (1982).
6. Sjollem, J.; Van Der Mei, H.C.; Uyen, H.M.; Busscher, H.J. "Direct Observa-

tions of Cooperative Effects in Oral Streptococcal Adhesion to Glass by Analysis of the Spatial Arrangement of Adhering Bacteria", *FEMS Microbiological Letters*, 69, pp. 263-270 (1990).

7. Schmidt, R. "Aggregation Kinetics of Saccharomyces Cerevisiae on Solid Surfaces", *Acta Biotechnologica*, 12, pp. 203-212 (1992).
8. Quirynen, M.; Marechal, M.; van Steenberghe, D.; Busscher H.J.; Van Der Mei, H.C. "The Bacterial Colonization of Intra-oral Hard Surfaces in Vivo: Influence of Surface Free Energy and Surface Roughness", *Biofouling*, 4, pp. 187-198 (1991).
9. Cressie, N.A.C. *Statistics for Spatial Data*, John Wiley & Sons Inc., New York, N.Y. (1991).
10. Ripley, B.D. *Spatial Statistics*, pp. 577-695, John Wiley & Sons Inc., New York, N.Y. (1981).
11. Diggle, P.J. *Statistical Analysis of Spatial Point Patterns*, Academic Press, New York, N.Y. (1983).
12. Hamilton, M.A.; Johnson, K.R.; Camper, A.K.; Stoodley, P.; Harkin, G.J.; Gillis, R.J.; Shope, P.A. "Analysis of Bacterial Spatial Patterns at the Initial Stage of Biofilm Formation", *Biometrical Journal* (1995, in press).
13. Cowan, M.; Busscher, H.J. "Flow Chamber Study of the Adhesion of Prevotella

Intermedia to Glass after Preconditioning with Mutans Streptococcal species: Kinetics and Spatial Arrangement", *Microbios*, 73, pp. 135-144 (1993).

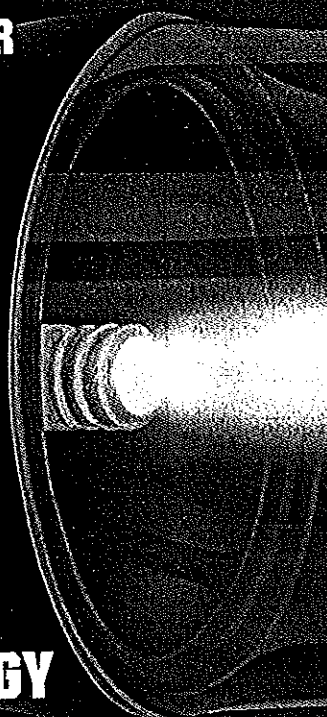
14. Busscher, H.J.; Noordmans J.; Meinders, J.; Van Der Mei, H.C. "Analysis of the Spatial Arrangement of Microorganisms Adhering to Solid Surfaces — Methods of Presenting Results", *Biofouling*, 4, pp. 71-79 (1991).

Authors Anne K. Camper, Department of Civil and Agriculture Engineering; Martin A. Hamilton, Ph.D., Department of Mathematical Sciences; Kirk R. Johnson, Department of Biology; Paul Stoodley, Center for Biofilm Engineering; Gary J. Harkin, Ph.D., Department of Computer Science; and Don S. Daly, Department of Mathematical Sciences may be contacted through the Center for Biofilm Engineering, 409 Cobleigh Hall, Montana State University, Bozeman, MT 59717; 406/994-4770.

This paper was presented at ULTRAPURE WATER Expo '94, May 9-11, 1994, Philadelphia, Pa.

**Key words:** BACTERIAL COLONIZATION, BIOFILM, FLOW CELL, IMAGE ANALYSIS, MICROSCOPY, SPATIAL POINT PATTERN ANALYSIS, STATISTICAL ANALYSIS

**SIMPLIFY YOUR  
APPROACH TO  
ULTRAVIOLET  
WATER  
PURIFICATION  
WITH  
HIGH  
ENERGY  
UV  
TECHNOLOGY**



**DISCOVER THE REAL SOLUTION TO:**

- Bacteria Control • TOC Reduction
- Ozone Destruct • High Temperature D.I.

**AQUIONICS**

INCORPORATED  
P.O. BOX 18395 • 21 Kenton Lands Road  
Erlanger, KY 41018  
Tel: (606) 341-0710 • Fax: (606) 341-2302

**WORLD  
LEADERS IN  
ULTRAVIOLET  
TECHNOLOGY**

**HANOVIA UV**

Hanovia Ltd, 145 Farnham Road, Slough,  
Berkshire SL1 4XB, England  
Tel: +44 (0) 753-812145  
Fax: +44 (0) 753 812191

